



Estd. 1989

JOURNAL OF ULTRA SCIENTIST OF PHYSICAL SCIENCES
 An International Open Free Access Peer Reviewed Research Journal of Physical Sciences
 website:- www.ultrascientist.org

Photo Response Studies of Electrophoretically Deposited Nanostructured Cadmium Sulfide Thin Film

ANEESH GEORGE^{1*} and M. ABDUL KHADAR²

¹Department of Physics, Mar Ivanios College, Thiruvananthapuram 695015, India

²Department of Nanoscience and Nanotechnology, University of Kerala, Thiruvananthapuram 695581, India

*Corresponding Author E-mail: aneeshndlphy@gmail.com, Ph: +91 9562260042

<http://dx.doi.org/10.22147/jusps-B/290401>

Acceptance Date 3rd March, 2017,

Online Publication Date 2nd April, 2017

Abstract

Cd²⁺ rich Cadmium Sulfide (CdS) nanoparticles capped with Triethanolamine (TEA) as an organic ligand were synthesized by chemical precipitation. These nanostructured CdS nanoparticles were deposited on aluminum foil by electrophoretic deposition technique. Both nanoparticles and thin film are studied by x-ray diffraction, glancing incidence x-ray diffraction and atomic force microscopy measurements to understand the growth, stability and surface morphology. The highest photocurrent obtained as 6.5 μ A at incident wavelength $\lambda = 400$ nm with an applied bias voltage of 10 V in the CdS thin films. Also time response of the photocurrent reveals the corrosion at the surface of CdS particles i.e get decompose into Cd²⁺ and S²⁻ ions.

Key words : Cadmium Sulfide, photocurrent, electrophoretic deposition.

Introduction

Cadmium sulfide is a direct band gap II-IV semiconductor ($E_g = 2.42$ eV) having useful optoelectronic properties and is being used in both photosensitive and photovoltaic devices. The electrophoretic deposition technique is widely explored, since it is particularly useful in film deposition of semiconductors, ceramic and organoceramic materials on cathodes from colloidal dispersions. Electrophoretic deposition is essentially a two-step process. In the first step, particles suspended in a liquid are forced to move toward an electrode by applying an electric field to the suspension (electrophoresis). In the second step, the particles collect at one of the electrodes

and form a coherent deposit on it¹. The deposition process yields only a powder compact, and therefore electrophoretic deposition should be followed by a densification step such as sintering or curing in order to obtain a fully dense material.

The photoconductivity of CdS in CdS/CdTe solar cells using the techniques spectral sensitization of apparent quantum efficiency (AQE) and explained the electrical property of CdS using current density-voltage analysis². Dark and photoresistances of 400 nm thick CdS films deposited using RF magnetron sputtering was approximately 1×10^5 and 3×10^4 Ω /sq, respectively³. Electrical conductivity of RF magnetron sputtered CdS films as a function of film thickness and temperature, and the conductivity was controlled by a thermally activated mobility in the presence

of an intergrain barrier⁴. Photoconductance in polycrystalline CdS films using conductance atomic force microscopy and found that photoconductivity along the grain boundaries was excited at photon energies significantly smaller than the band gap of CdS, whereas phototransport through the grains was detected only for photon energies above band gap⁵. Adsorption of oxygen caused reduction of photocurrent in CdS nanoribbons. This result was in accordance with the strong bonding of oxygen with sulfur defect states⁶. In CdS plates decay of photocurrent took place for light energy higher than the band gap of CdS due to the photoinduced surface dissolution of CdS⁷. In this paper, we report the preparation, characterization and Dark and photo current variations of nanostructured cadmium sulfide thin films.

Experimental

Nanoparticles of CdS with Cd²⁺ rich surface were synthesized through Sol-Gel method. Required amount of cadmium acetate and sodium sulfide dissolved in 10 ml of distilled water respectively, were dropped simultaneously in to distilled water mixed with 1M Triethanolamine (TEA) as capping agent kept stirred using a magnetic stirrer in a conical flask. The surface of CdS nanoparticles formed adsorbed the excess Cd²⁺ cations. The nanoparticles of CdS were separated by centrifugation, washed repeatedly using distilled water and then in acetone. The sample was then dried.

Nanostructured films of CdS were deposited on aluminum substrate by electrophoretic deposition technique. For deposition, nanoparticles of CdS were dispersed in distilled water using ultrasonic disintegrator. Aluminum plates of purity 99.99% and of size 1×2 cm were used as electrodes. The electrodes were dipped in a suspension of CdS nanoparticles at a separation of 2 cm. A potential difference was applied between the electrodes using a voltage source. The potential difference was adjusted in such a way that the current through the CdS suspension was 3 mA. CdS film appeared on the cathode. Then the film washed well with distilled water and then air dried. The film samples used for electrical measurements were annealed at 120 °C for 30 minutes.

X-ray powder diffraction (XRD) of the CdS nanoparticles were performed using XPERT-PRO diffractometer with Cu K α radiation ($\lambda = 1.5406 \text{ \AA}$), employing a scanning rate of $0.05^\circ \text{ s}^{-1}$ in the 2θ range from 15° to 70° . Glancing incidence X-ray diffraction (GIXRD) analysis of the nanostructured CdS thin films was carried out using a BRUKER AXS D8 diffractometer with Cu K α radiation, employing scanning rate $0.05^\circ \text{ s}^{-1}$ in the 2θ range

from 20° to 70° with 0.5° and 1° incident angles. Atomic force microscopy (AFM) observations were carried out on the film samples using a NANOSCOPE-E in contact mode. Photo current measurements were carried out using PHILIPS 100W bulb as light source. The wavelength response of photocurrent was measured over the wavelength range from 250 to 600 nm using a 1000 W Xenon lamp as source and a monochromator. The rise and decay of photocurrent was recorded using a TEKTRONIX TDS 1012B storage oscilloscope along with KEITHLEY 2400 source meter and a computer.

Results and Discussion

A typical XRD pattern of CdS nanoparticles is shown in figure 1. The broad peaks in the XRD pattern indicate that the CdS samples consisted of nanometer sized particles. The peaks centered at 2θ values of 26.63° , 44.02° and 52.20° could be attributed to the reflection from (111), (220) and (311) planes of cubic phase of CdS in comparison with the ICDD file for cubic CdS (file No: 06-0314) and reported results⁸.

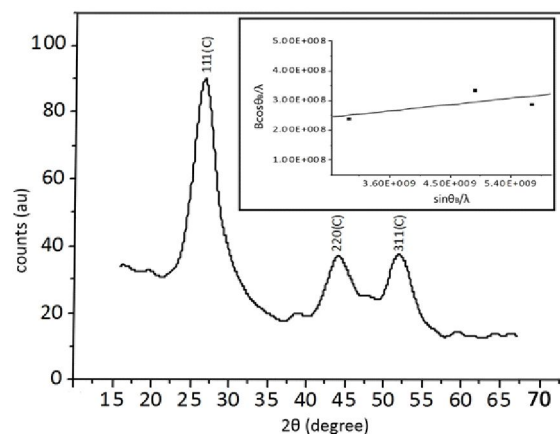


Figure 1 XRD pattern of nanoparticles of CdS inset Hall Williamson plot

The size of the nanoparticles of CdS was calculated from the broadening of peaks in the XRD pattern using the Debye-Scherrer formula and is obtained as 3.19 nm. The particle size after eliminating broadening of the peaks due to microstrain was determined making use of the Hall Williamson relation. The size of the CdS nanoparticles obtained from the Hall-Williamson plot shown as insight to figure 1 was 3.6 nm.

Figure 2 shows the GIXRD pattern of as-prepared CdS film samples recorded for an incident angle of 0.5° . The

pattern exhibits peaks corresponding to the cubic phase of CdS along with the peaks of the aluminum substrate which is in good agreement with the XRD result of CdS nanoparticles.

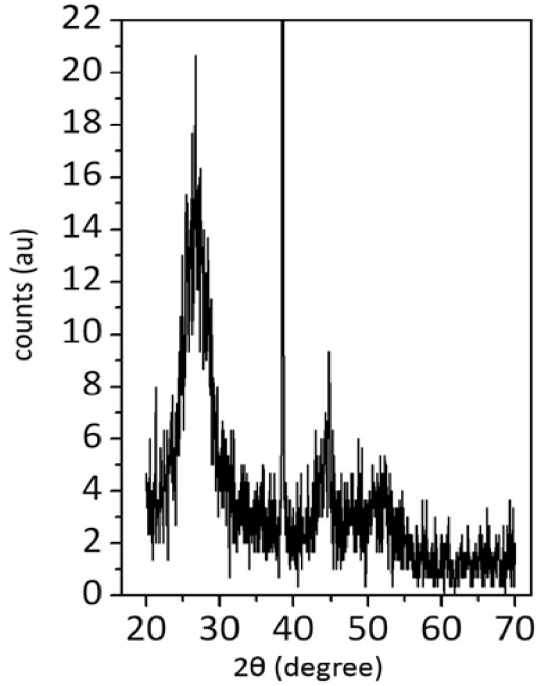


Figure 2 GIXRD pattern of CdS film at an incident angle of 0.5°

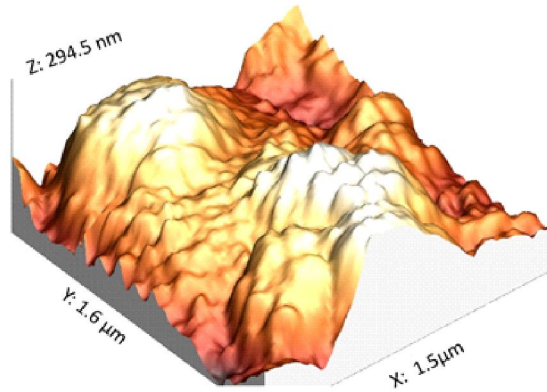
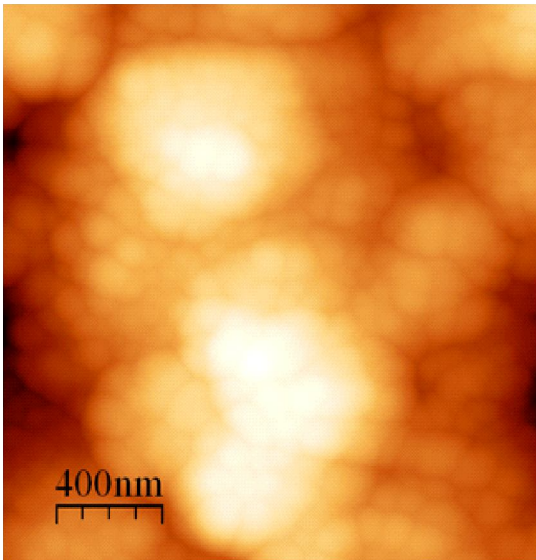


Figure 3(a) Surface morphology (b) 3D view of CdS film

Figure 3 shows the AFM image of the CdS film. In electrophoretic deposition, the particle size does not change but agglomeration can take place during deposition as shown in the AFM images. The average size of the agglomerate determined from the AFM image was 100 nm. Thus the nanostructured film of CdS consisted of agglomerates of primary CdS nanoparticles.

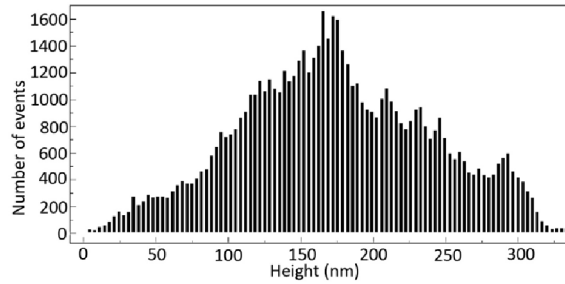


Figure 4 Height histogram

Roughness of the surface of the nanostructured films is a parameter of interest in relation to gas absorption, corrosion, or optical surface quality. With AFMs, the interaction force between the probing tip and the sample is very small and the spatial resolution is high. The RMS roughness, R_{rms} , of the film is given by the standard deviation of the data,

$$R_{rms} = \sqrt{\frac{\sum_{n=1}^N (z_n - \bar{z})^2}{N - 1}}$$

where \bar{z} is the average of the height of the film surface within the given area, z_n is the current height, and N is the number of data points within the given area⁹. The mean roughness

or the peak-to-valley distance are less accurate than the RMS roughness. The RMS value was also calculated from the phase shift θ_{rms} by the equation

$$\theta_{rms} = \sqrt{\frac{\sum_{n=1}^N (\theta_n - \bar{\theta})^2}{N - 1}}$$

where $\bar{\theta}$ is the average of the θ values within the given area, θ_n is the current θ value, and N is the number of data points within the given area¹⁰. Figure 4 shows the number of events versus height histogram of the CdS thin film deposited on the Al substrate. In the given area a large height distribution was observed. This distribution was used to calculate the roughness of the samples. The R_{rms} value of roughness of the film samples was obtained as 66 nm.

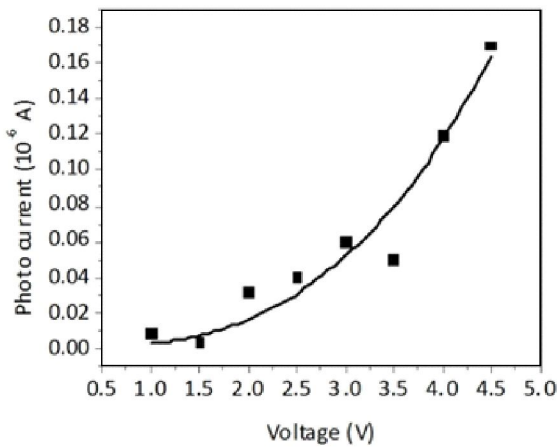
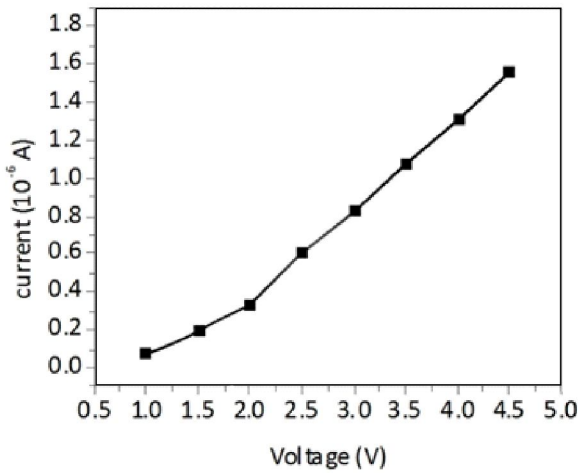


Figure 5 variations of current with applied voltage of nanostructured CdS thin film deposited on Al substrate (a) dark current and (b) photocurrent.

The band gap energy of CdS is in the energy range of visible light and the photosensitivity in the visible range is high for CdS thin films. Photoconductive materials generally exhibit spectral distribution curves having more or less sharp peaks in the vicinity of the absorption edge¹¹. The photocurrent (I_{ph}) is given by $I_{ph} = I_L - I_D$, where I_L and I_D are current under illumination and dark current respectively¹². Figure 5(a) shows the I-V characteristics in dark and in the presence of light for CdS film. The photocurrent of CdS thin films for different applied voltages is shown in figure 5(b).

The variation of photocurrent with wavelength of incident light observed at an applied bias voltage of 10 V in the CdS thin films is shown in figure 6. As the energy of the incident light increased, photocurrent increased sharply reaching a peak value around $\lambda = 400$ nm. The photocurrent increased from a value of 0.3 μ A at $\lambda = 550$ nm to a value of 6.5 μ A at $\lambda = 400$ nm.

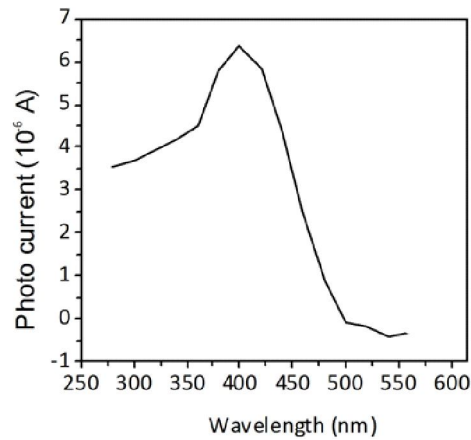


Figure 6 Photo current for an applied voltage 10 V as a function of wavelength of incident light.

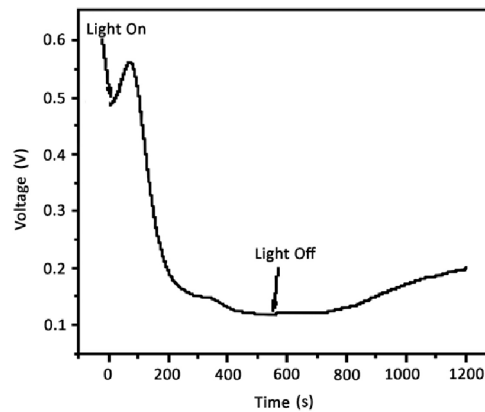


Figure 7 Time response of CdS film

The photocurrent rise and decay characteristics are important aspects for characterization of defects in a film. The defects act as deep trap states situated at different energy depths within the forbidden gap and thereby influence the photo response of the sample. Time response of the nanostructured CdS thin film sample is shown in figure 7. For a fixed voltage across the electrodes in dark, a steady current will flow in the circuit. The initial fast rise of photocurrent in the presence of light is due to the increase of number of charge carriers. However, after equilibrium a slow retrapping process starts where the holes from the valence band are trapped at hole centers. Therefore, an equivalent number of electrons are added to the conduction band that results in a slow rise of current on further illumination. There are three possible reactions for the holes in CdS. First, the positive holes could result in CdS dissolution. Second, they may directly oxidize organic compounds if strong absorption occurs and the reaction is thermodynamically favorable. Third, they may react with adsorbed H_2O and OH^- to produce hydroxyl radicals if either organic adsorption is insignificant or the reaction is thermodynamically unfavorable for direct charge transfer. Therefore, illumination causes oxidization of CdS particles leading to an exponential decrease of photocurrent. Thus the decrease of photocurrent is due to the corrosion at the surface of CdS particles.

Conclusion

Electrophoretically deposited CdS thin film on aluminum substrate was nanostructured. The particle size of CdS nanoparticles calculated from XRD pattern and Hall Williamson plot were 3.1 and 3.6 nm respectively. As-prepared CdS thin film was highly amorphous so that broad peak occurs in GIXRD. The photo current was observed in the order of micro ampere. Electrophoretic deposited film is highly porous and less grain boundary merging, because each particle behaves as single particle. In the presence of oxygen, the conductivity of the CdS film decreases. So CdS thin film can be act as an oxygen sensor.

References

1. S. Frank, C. Mochales, M. Heimann, F. Kochbeck, R. Zehbe, C. Fleck and W.D. Mueller, Electrophoretic Deposition of zirconia nanoparticles, *Nanosci Technol* 1(1): 5 (2014).
2. S. Hegedus, D. Ryan, K. Dobson, B. McCandless and D. Desai, Photoconductive CdS: how does it Affect CdTe/CdS Solar Cell Performance?. *Mat. Res. Soc. Symp. Proc.* 763: B9.5 (2003).
3. S.G. Hur, E.T. Kim, J.H. Lee, G.H. Kim and S.G. Yoon, Characterization of photoconductive CdS thin films prepared on glass substrates for photoconductive-sensor applications. *J. Vac. Sci. Technol. B* 26(4): 1334 (2008).
4. F.E. Akkad and H. Ashour, Photoinduced current transient spectroscopy technique applied to the study of point defects in polycrystalline CdS thin films. *J. Appl. Phys.* 105: 093113 (2009).
5. D. Azulay, O. Millo, S. Silbert, and I. Balberg, Where does photocurrent flow in polycrystalline CdS? *Appl. Phys. Lett.* 86, 212102 (2005).
6. J.S. Jie, W.J. Zhang, Y. Jiang, X.M. Meng, Y.Q. Li, and S.T. Lee, Photoconductive Characteristics of Single-Crystal CdS Nanoribbons. *Nano Lett.* 6(9), 1887-1892 (2006).
7. A.J. Frank, S. Glenis, and A.J. Nelson, Conductive polymer-semiconductor junction: characterization of poly(3-methylthiophene): cadmium sulfide based photoelectrochemical and photovoltaic cells. *J. Phys. Chem.* 93, 3818-3825 (1989).
8. A.M.A. Al-Hussama, S.A.J., Jassim, Synthesis, structure, and optical properties of CdS thin films nanoparticles prepared by chemical bath technique, *J. Assoc. Arab Univ. Basic Appl. Sci.*, 11(1): 27-31 (2012).
9. S.V. Kamat, V. Puri, and R. K. Puri, The Effect of Film Thickness on the Structural Properties of Vacuum Evaporated Poly(3-methylthiophene) Thin Films, *Inter. Schol. Research Network ISRN Polymer Science*, Article ID 570363, 8 pages (2012).
10. K. Boussu, B.V.D. Bruggen, A. Volodin, J. Snauwaert, C.V. Haesendonck, C. Vandecasteele, Roughness and hydrophobicity studies of nanofiltration membranes using different modes of AFM. *J. Coll. Inter. Sci.* 286, 632-638 (2005).
11. M.Y. Han, W. Huang, C.H. Quek, L.M. Gan, C.H. Chew, G. Xu, and S.C. Ng, Preparation and enhanced photocatalytic oxidation activity of surface-modified CdS nanoparticles with high photostability. *J. Mater. Res.* 14(5), 2092-2095 (1999).
12. A. Kisiel, B. Pukowska, W. Tomkowicz, S.A. Ignatowicz and B.S. Nowak, Optical properties of ZnTe thin films. *Thin Solid Films*, 34, 399-402 (1976).